

CIRCULATION COPY
SUBJECT TO RECALL
IN TWO WEEKS

UCID- 18500

Lawrence Livermore Laboratory

NOZZLE MODEL OF FLOWING PLASMA WITH FIELD REVERSAL

J. W. Shearer

January 7, 1980



DISCLAIMER

This document was prepared as an account of work sponsored by an agency of the United States Government. Neither the United States Government nor the University of California nor any of their employees, makes any warranty, express or implied, or assumes any legal liability or responsibility for the accuracy, completeness, or usefulness of any information, apparatus, product, or process disclosed, or represents that its use would not infringe privately owned rights. Reference herein to any specific commercial product, process, or service by trade name, trademark, manufacturer, or otherwise, does not necessarily constitute or imply its endorsement, recommendation, or favoring by the United States Government or the University of California. The views and opinions of authors expressed herein do not necessarily state or reflect those of the United States Government or the University of California, and shall not be used for advertising or product endorsement purposes.

This report has been reproduced
directly from the best available copy.

Available to DOE and DOE contractors from the
Office of Scientific and Technical Information
P.O. Box 62, Oak Ridge, TN 37831
Prices available from (615) 576-8401, FTS 626-8401

Available to the public from the
National Technical Information Service
U.S. Department of Commerce
5285 Port Royal Rd.,
Springfield, VA 22161

NOZZLE MODEL OF FLOWING PLASMA WITH FIELD REVERSAL*

J. W. Shearer

ABSTRACT

The flowing plasma outflow from a field-reversed plasma gun is modeled by a one-dimensional calculation which is based on the well-known problem of fluid flow through a nozzle. The results suggest that a low plasma mass flow rate is necessary for reconnection to be important. Comparison with 2D MHD calculations and with preliminary data from the BETA-II experiment are consistent with the model at this time.

INTRODUCTION

2D MHD code calculations have shown that the plasma emitted by a "Marshall gun" is many times longer than its radius. These results include cases where field reversal has been imposed on the plasma. The high axial velocity of these plasmas suggests that a useful model could be constructed by analogy with flow through a nozzle, because a magnetic field coil channels the plasma flow in a manner similar to the walls of a nozzle.

This is a 1D calculation which applies these ideas to the question of magnetic diffusion through the plasma layer. Results obtained from the 1D calculation are then used to discuss the 2D reconnection problem and to compare with the BETA-II experiment.

MAGNETIC FLUX

Consider a sharp boundary model of a long plasma at radius r of thickness $2a \ll r$. The magnetic field has the magnitude B both inside and outside the plasma, but its direction is reversed inside the plasma. Now apply Faraday's Law:

$$-\dot{\phi}_i = V = \int \epsilon_\theta r d\theta \approx 2\pi r \eta J_\theta \approx 2\pi r D \frac{B}{a} \quad (1)$$

where ϕ_i is the inside flux $\pi r^2 B$, V is the loop voltage, ϵ_θ is the electric field, J_θ is the average current density, and $D = \eta/\mu$ is the diffusivity (where η = resistivity and μ = magnetic permeability). We have assumed a linear variation of B through the plasma layer.

This whole system is contained inside a conducting wall of radius, R , in which the total flux ϕ_T is given by:

$$\phi_T = \phi_o + \phi_i - \phi_i = \phi_o \quad (2)$$

where ϕ_o is the open field line flux outside the field-reversed region. Assuming pressure equilibrium and remembering that $2a \ll r$, one has:

$$\phi_o + \phi_i = \pi(R^2 - r^2)B \quad (3)$$

$$\phi_i = \pi r^2 B \quad (4)$$

As diffusion proceeds, ϕ_i will change with time according to Eq. (1). As the plasma flows under a magnetic coil, the open field line flux ϕ_o will also change in time. Both of these changes will affect the values of r and B .

One useful relation is found by eliminating ϕ_i from Eqs. (3) and (4) to obtain an equation for r :

$$r = \frac{R}{\sqrt{2}} \left(1 - \frac{\phi_o}{\pi R^2 B} \right)^{1/2} \quad (5)$$

More useful yet is the solution for B which is obtained by eliminating r from the same two Eqs. (3) and (4):

$$B = \frac{1}{\pi R^2} (\phi_o + 2\phi_i) \quad (6)$$

As the plasma flows under the coil, the changes in B can be computed from the changes in ϕ_i . Eq. (1) and the changes in the external flux ϕ_o . In this model the independent variable is chosen to be the axial coordinate Z , rather than the time t . Furthermore, the magnetic pressure $P = B^2/2\mu$ is chosen as the most useful dependent variable, because it is simple to equate this to the plasma pressure inside the layer. Thus one has from Eq. (6):

$$P = \frac{1}{2\pi^2 \mu R^4} (\phi_o + 2\phi_i)^2 \quad (7)$$

For the variation in Z , one gets:

$$\frac{1}{P} \frac{dP}{dZ} = \frac{2}{\phi_o + 2\phi_i} \left(\frac{d\phi_o}{dZ} + 2 \frac{d\phi_i}{dZ} \right) \quad (8)$$

Use Eq. (1) to find:

$$\frac{d\phi_i}{dZ} = \frac{1}{u} \phi_i = - 2\pi \frac{rD}{ua} \sqrt{3\mu P} \quad (9)$$

where $u = dZ/dt$ is the plasma velocity. The changes in the open field flux ϕ_o are independently specified. The calculations reported here use a polynomial expression:

$$\phi_o = 4\phi_m \left[\frac{Z}{Z_o} - \left(\frac{Z}{Z_o} \right)^2 \right] \quad (10)$$

where Z_o is the total axial distance in the calculation, and ϕ_m is the maximum value of ϕ_o , which occurs at $(Z/Z_o) = 0.5$. Note that for this case $\phi_o = 0$ both at the starting point ($Z = 0$) and the end point ($Z = Z_o$). Now differentiate:

$$\frac{d\phi_o}{dZ} = \frac{4\phi_m}{Z_o} \left(1 - 2 \frac{Z}{Z_o} \right) \quad (11)$$

Finally, by combining Eqs. (7), (8), (9), and (11), one obtains the desired differential equation:

$$\frac{dP}{dZ} = \sqrt{\frac{2P}{\mu}} \frac{4\phi_m}{\pi R^2 Z_o} \left(1 - \frac{2Z}{Z_o} \right) - \frac{8rDP}{uaR^2} \quad (12)$$

This is the fundamental equation of the model. The first term is the "nozzle" term — that is, it relates the change in pressure of the flowing plasma to the input constants, ϕ_m , R of the "coil," centered at $Z = Z_o/2$. The second term is the diffusion term, as derived from Eq. (1). The total pressure is lowered by the diffusion because ϕ_i is reduced.

To complete the description of the flow, one has to adopt a model for the plasma in order to specify the diffusivity D , the velocity u , and the plasma thickness a . A particular plasma model is discussed in the next section.

PLASMA MODEL

The hydrogen ($Z = 1$) plasma has a low electron temperature T_e and a moderate-to-high ion temperature T_i ($T_e \ll T_i$). Thus, electron pressure is neglected compared to ion pressure. Furthermore, the electron temperature is assumed to be constant in time and distance, because its large thermal conductivity equalizes the temperature effects of compression and rarefaction. On the other hand, the ions are modeled by an adiabatic fluid with specific heat ratio γ , stagnation pressure P_s , and maximum velocity

U_m . This allows us to make direct use of the well-known equations for compressible flow through nozzles.¹

Using the adiabatic and Bernoulli equations, it can be shown that the stagnation density ρ_s is:

$$\rho_s = \frac{2\gamma}{\gamma-1} \frac{P_s}{U_m^2} \quad (13)$$

Then the adiabatic law is used to find the actual density ρ :

$$\rho = \rho_s (P/P_s)^{1/\gamma} \quad (14)$$

The actual velocity u can be found from the "Saint-Venant and Wantzel" equation:

$$u = U_m \left[1 - \left(\frac{\rho}{\rho_s} \right)^{\frac{\gamma-1}{\gamma}} \right]^{1/2} \quad (15)$$

Combining Eqs. (14) and (15) yields a convenient alternative form for the velocity u :

$$u = U_m \left[1 - \left(\frac{\rho}{\rho_s} \right)^{\gamma-1} \right]^{1/2} \quad (16)$$

The plasma thickness parameter $2a$ is a function of the mass flow rate F , which is an input parameter of the model:

$$a = F/(4\pi r_{up}) \quad (17)$$

Thus, all of the hydrodynamic characteristics of the plasma flow are accounted for by this adiabatic model of the plasma ions.

The magnetic diffusivity $D = \eta/\mu$ is separately treated because it is a different function of the plasma parameters. The basis for this model is the classical collisional electrical resistivity² η_o , which can be approximated by:

$$\eta_o = 100/(T_e)^{3/2} \quad (18)$$

where η_o is in $\mu\text{sec-emu}$ units, and the electron temperature T_e is in eV.

A heuristic correction for anomalous resistivity is incorporated in the model by writing:

$$\eta = \eta_0 \exp (v_d/v_i)^2 \quad (19)$$

where v_d is the electron drift velocity, and v_i is the ion thermal velocity. This velocity ratio needs to be rewritten in another way:

$$\left(\frac{v_d}{v_i} \right)^2 = \frac{c^2 J^2}{e^2 n^2} \frac{2}{3} \frac{A M_H}{k T_i} \quad (20)$$

where A is the atomic weight, and M_H is the proton mass. Remember that:

$$B^2/2\mu = P \approx n k T_i \quad (21)$$

$$n = \rho/A M_H \quad (22)$$

Then from Eq. (1) and some algebra, one gets:

$$\left(\frac{v_d}{v_i} \right)^2 = \left[\frac{4}{3} \frac{(A M_H)^2}{\mu m r_o} \right] \frac{1}{\rho a^2} \quad (23)$$

where m is the electron mass and r_o is the classical electron radius e^2/mc^2 . For the case of a deuterium plasma, one has $A = 2$, and the constant in brackets is $4.625 \times 10^{-9} \text{ gm/cm}$.

Thus, at last one collects the results of Eqs. (18), (19), and (23) to arrive at the final expression for diffusivity D :

$$D = \left(\frac{25}{\pi} \right) \left(\frac{1}{T_e} \right)^{3/2} \exp \left(\frac{4.625 \times 10^{-9}}{\rho a^2} \right) \quad (24)$$

There is no allowance for saturation of the anomalous resistivity in this model because it is not believed to be an important effect. When the plasma width a becomes small enough to raise the diffusivity D , this lowers the pressure P [from Eq. (12)]. The consequences are that density ρ is lowered

[Eq. (14)], and the plasma width a is increased again [Eq. (17)]. Physically, the increased plasma width lowers the current density J and the drift velocity v_d , which stabilizes the sheath. Such stable plasma sheath widths have been known for some time.³

Eq. (24) for the diffusivity completes the plasma model.

CALCULATION PROCEDURE

For completeness the details of the calculational procedure are described here. First is a list of input constants and their values for the reference calculation:

Gamma	$\gamma = 5/3$
Maximum Velocity	$U_m = 100 \text{ cm/sec}$
Maximum Axial Distance	$Z_m = 200 \text{ cm}$
Wall Radius	$R = 20 \text{ cm}$
Plasma Mass Flow Rate	$F = 6 \times 10^{-6} \text{ gm/sec}$
Stagnation Pressure	$P_s = 2 \times 10^{-6} \text{ mb-cc}$
Initial Pressure	$P_o = 2.5 \times 10^{-7} \text{ mb-cc}$
Maximum Coil Flux	$\phi_m = \pi \text{ MG-cm}^2$
Electron Temperature	$T_e = 50 \text{ eV}$

The ideal gas law γ is used because the ions are always assumed to be fully ionized with a single isotropic temperature. The maximum velocity U_m corresponds to a deuterium ion energy of 10 keV, which is at the high end of the energy spectrum reported for most plasma guns. The axial distance Z_m and the wall radius R are similar to β -II experiment parameters. The plasma mass flow rate corresponds to a line density (at velocity U_m) of deuterium of 1.8×10^{16} ions/cm and an ion flow rate of 1.8×10^{18} ions/ μ sec. The desired initial field-reversal target plasma for the β -II experiment is 2.5×10^{18} ions,⁴ corresponding to about 1.4 μ sec at this flow rate. The stagnation pressure P_s corresponds to a magnetic field of about 7 kG; the starting pressure P_o to 2.5 kG. Thus, at $Z = 0$, $2\phi_1 = \pi \text{ MG-cm}^2 = \phi_m$, corresponding to a maximum magnetic field (under the coil at $Z = Z_m/2$) of 5 kG in the absence of any diffusion. This reference case is included in the results to be described below.

Two additional steps complete the startup procedure for each calculation. The stagnation density ρ_s is found from Eq. (13), and the pressure is initialized ($P = P_o$).

The calculation cycle follows this sequence: ρ [Eq. (14)], u [Eq. (16)], r [Eq. (5) with pressure P instead of field B]

$$r = \frac{R}{\sqrt{2}} \left(1 - \frac{\phi_o}{\sqrt{2\mu\pi r^2}} \frac{1}{\sqrt{P}} \right)^{1/2} \quad (25)$$

a [Eq. (17)], and D [Eq. (24)]. Then the pressure P is advanced to a new value $P + \Delta P$ at a new value of axial distance $Z + \Delta Z$ by means of the basic differential equation [Eq. (12)], using the "GEAR" package for numerical stability.⁵ Finally, the accumulated time τ for the plasma flow to reach this value of Z is kept track of:

$$\tau = \int_0^Z \frac{dZ}{u} \cong \sum \frac{\Delta Z}{u} \quad (26)$$

This completes one cycle, and the calculation goes back to the beginning of this paragraph to start the new cycle.

The usual condition for termination of the calculation is when $Z \geq Z_m$, that is, when the axial distance has reached the end of the coil. An alternative condition for ending the calculation is if $a \geq r$, a condition which is an obvious violation of the very first assumption of the model ($2a \ll r$).

The output of the calculation is numerical; all of the important parameters are given for $Z = 0$ and for 20 evenly-space values of the axial distance Z .

RESULTS

The reference calculation gave the results plotted in Fig. 1. One sees the radius r of the plasma shrink as it passes under the coil centered at $Z = 100$ cm. The magnetic field B increases to a maximum of 4.28 kG at that point, which is less than the 5 kG value it would have had in the absence of the field diffusion term. This diffusion directly affects the inner flux ϕ_i , and indeed ϕ_i declines throughout the flow. Due to this decline, the final value of B (1.54 kG) is less than its initial value (2.50 kG). This lower pressure lowers the plasma density ρ , and increases the plasma sheath

thickness $2a$ and velocity u . Note also how u slows down under the coil where the pressure is maximum.

Finally, an especially interesting result is that the rate of change of the flux ϕ_i is greatest in the low pressure regions at the beginning and end of the problem, and it is almost negligible in the high pressure, high density region under the coil center ($Z = 100$ cm). Another aspect of this same phenomenon appears in Fig. 2, where the reference calculation is compared to other cases with different mass flow rates F . Comparatively small changes in the flow rate make large differences in the flux leakage and the pressure. At $F = 10^{-5}$ there is almost no flux loss, as evidenced by the maximum pressure being almost one atmosphere (corresponding to 5 kG). For the lowest values of F the effects of diffusion are strongly felt, especially in the low pressure regions near $Z = 0$ and $Z = 200$. For $F = 5 \times 10^{-5}$, the pressure actually drops at the start of the calculation, an extreme example of this low pressure diffusion.

The explanation for the low pressure effect is more apparent in Fig. 3, which is a plot of the plasma half-thickness a and the magnetic diffusivity D versus the flow parameter F in the low pressure region near the start of the flow ($Z = 10$). The half-thickness a is only a weak function of the flow F , but the diffusivity D varies strongly with F because of the exponential term in Eq. (24). Thus, the anomalous resistivity effects that stabilize the sheath will strongly enhance the magnetic diffusion for cases where the plasma density is low enough to approach the noncollisional state. This enhancement continues until the field drops to a low enough value to permit the sheath to broaden, thus lowering the field gradient and the drift velocity.

Fig. 4 is a graph of the inner fluxes ϕ_i at the two extreme ends of the problem ($Z = 10$ and $Z = 200$) plotted versus the flow parameter F . At the lowest flow rate ($F = 5 \times 10^{-6}$) one again finds a large drop in ϕ_i at the very beginning of the flow, for the same reason as just described. At intermediate values of F the flux loss is more generally dispersed over the entire flow. At the highest flow rate ($F = 10^{-5}$) there is little flux loss at all, as was previously noted in Fig. 2. Thus, there is a fairly narrow range of flow rates in which one sees a general diffusion of flux from one end of the problem to the other. However, Fig. 1 still shows that the major flux losses occur in the comparatively low pressure regions of the flow.

Higher pressure effects were studied next by raising the input value of the maximum coil flux to $\phi_m = 2\pi \text{ MG-cm}^2$, instead of its input value of π . All other input constants remained unchanged, except for various choices of the flow rate F . Fig. 5 is a plot of the pressure versus time history of three of these runs. Only the lowest flow rate ($F = 5 \times 10^{-6} \text{ gm}/\mu\text{sec}$) gave a complete solution. The higher flow rates terminated when the half-thickness a exceeded the radius r . The reason for this was that the plasma pressure was approaching so close to the stagnation pressure P_s that the velocity u was approaching zero and the plasma was piling up. This effect is shown graphically in Fig. 6 for $F = 6 \times 10^{-6} \text{ gm/sec}$ (the same flow rate as for the reference case shown in Fig. 1). The physical interpretation of this result is that a very high coil pressure can stop the plasma by stagnating it against the mirror field. The lowest flow rate case escaped stagnation only because it lost sufficient inner flux to lower the overall pressure below the stagnation value P_s . In Fig. 5 the pressure P_m is the value the pressure would have reached in the absence of magnetic diffusion for a plasma with a higher stagnation pressure.

COMPARISON WITH 2D MHD CALCULATION

The results just described are an aid to the interpretation of the more elaborate two-dimensional magnetohydrodynamic calculations of field-reversed plasma production. Fig. 7 is a selection of output pictures from the most successful of these 2D calculations done to date.⁶ The output from the plasma gun is forced to flow through a passive conducting aperture, and then through a "pulsed coil" aperture. The latter aperture is similar to the one mocked up in the 1D NOZZLE model calculations just described, but it differs from it by being time-dependent. The flux is stronger at $t = 11.2 \mu\text{sec}$ than at $t = 10.8 \mu\text{sec}$.

The ra_θ plots are essentially poloidal field flux line plots, and they show that the flowing field-reversed plasma is very much elongated, similar to the NOZZLE calculations. Evidence for diffusion is seen at the later time ($t = 11.2 \mu\text{sec}$) where one of the field lines has reconnected. But note that the reconnection region is not located under the pulsed coil, but downstream from it. The velocity vectors (\vec{u}) in the bottom plot of Fig. 7 show a marked

speedup in the flow in the reconnection region and virtual plasma stagnation upstream from the pulsed coil. This behavior is also in qualitative agreement with the NOZZLE model calculations which showed enhanced diffusion in lower pressure higher flow velocity regimes.

The time-dependent pressure increase under the pulsed coil in the 2D problem should enhance the reconnection process by steepening the axial velocity gradient, because the later portions of the plasma flow will be slowed down more dramatically by the increased plasma pressure. Thus the flow rate parameter F , which was assumed to be a constant in the NOZZLE calculations, will become time-dependent, and will decrease just downstream from the pulsed coil. But the NOZZLE calculations show that the diffusion rate can increase dramatically when F is decreased. This effect reinforces the tendency to reconnect downstream from the pulsed coil.

Thus the two calculations are in basic agreement with each other, and present a consistent picture of the behavior of the field-reversed plasma emerging from the plasma gun.

COMPARISON WITH PRELIMINARY BETA-II DATA

There is only a small amount of data thus far available from the BETA-II experiment. Field reversal has been seen on axis, and the field-reversal plasma formation persists for 5 to 10 μsec . Both of these observations are consistent with the NOZZLE model, which assumes a constant plasma flow, and which calculates that field reversal is maintained over a 2-meter length.

Data on density and flow velocity would be of especial interest to compare with these models, if it were available.

SUMMARY

On the basis of these studies, the following conclusions have been reached about the reconnection problem in the flowing plasma outflow from a field-reversed plasma gun setup.

First, for the usual BETA-II flow rates and magnetic fields the plasma is dense enough to be dominated by collisional resistivity, and thus it will not diffusively reconnect on a short 1 to 10 μsec time scale.

Second, for somewhat lower flow rates, pressures, and/or densities, anomalous effects will try to increase the plasma resistivity. However, the resultant effect for high beta plasmas is to increase the current sheath width, thereby stabilizing the effect.

Third, appreciable magnetic diffusion and reconnection will occur on the BETA-II time-scale only when this anomalous effect is important -- namely, at low plasma flow rates.

Fourth, compression of the flow by a clipper coil does not directly produce reconnection. Instead, it slows down the velocity, which tends to thicken the plasma. It increases the density, which tends to make the plasma more collisional.

Fifth, the clipper coil compression can produce reconnection by various indirect means. It can stagnate the later portions of the flow, thereby opening up a low density, low flow rate region where the anomalous effect can speed up reconnection. Even if it does not completely stagnate the flow, a time-dependent compression can enhance the axial velocity gradient and reduce mass flow rate F just downstream from the clipper.

Sixth, reconnection would be a simpler problem if the plasma outflow from the plasma gun were a sharp pulse in flow rate F , rather than the long drawn-out flow that it seems to be at present.

Seventh, preliminary data from the BETA-II field reversal experiment are consistent with these calculations, but much additional data are needed for a detailed comparison.

REFERENCES

1. See Eq. 1-17, p. 13 of E.R.C. Miles, "Supersonic Aerodynamics," Dover Publications, New York (1961).
2. Eq. 5-42, p. 143 of Lyman Spitzer, "Physics of Fully Ionized Gases," 2nd Ed. Interscience, New York (1962).
3. S. Hammsaki, et al., Nuclear Fusion 14, 27 (1974).
4. T. C. Simonen, et al., "Plasma Gun Proposal," p. 15 of LLL Prop-156, August 18, 1978.
5. A. C. Hindmarsh, LLL Report UCID-30001, Rev. 3 (December 1974).
6. James Eddleman, private communication.

jbs

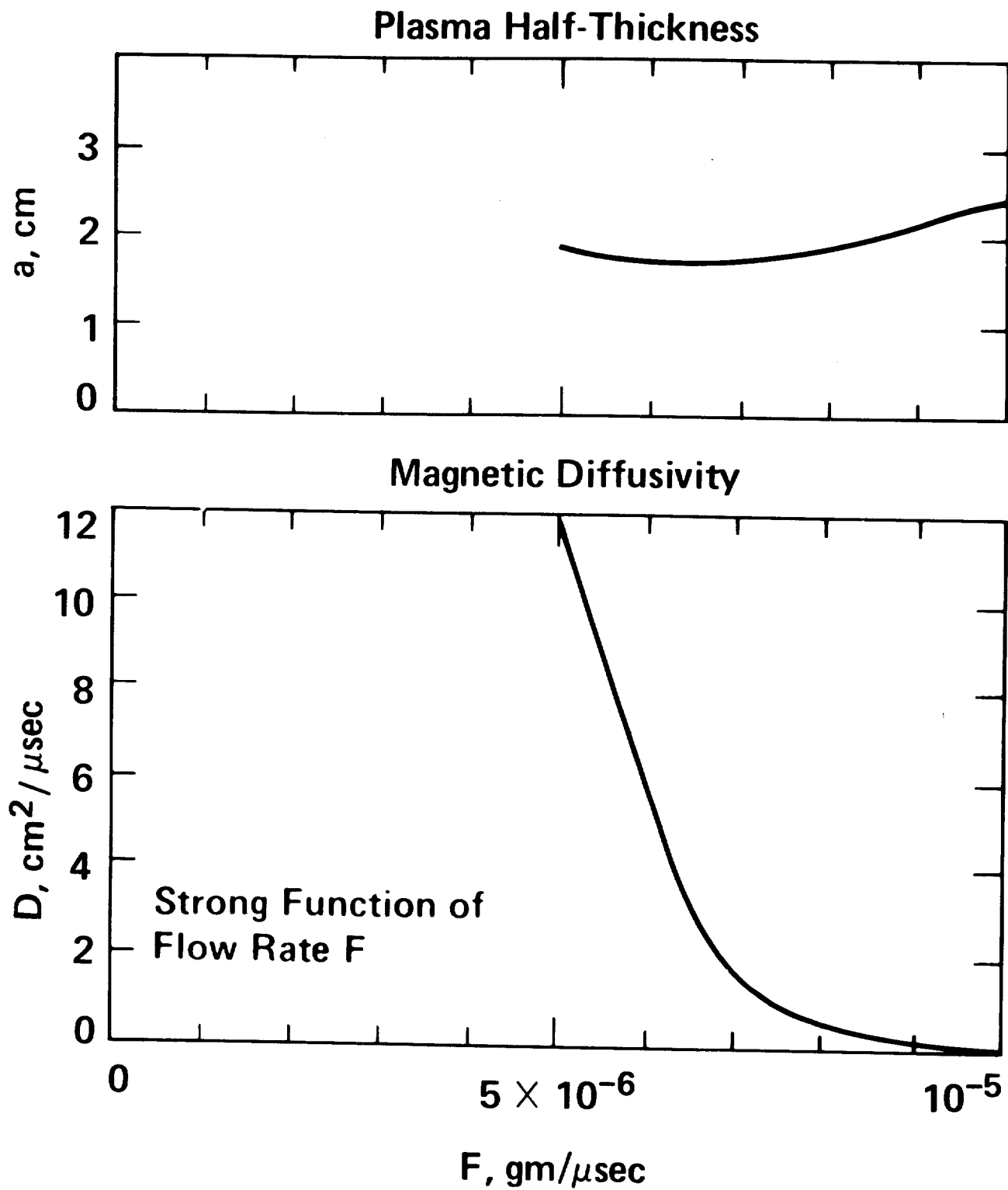


Figure 3

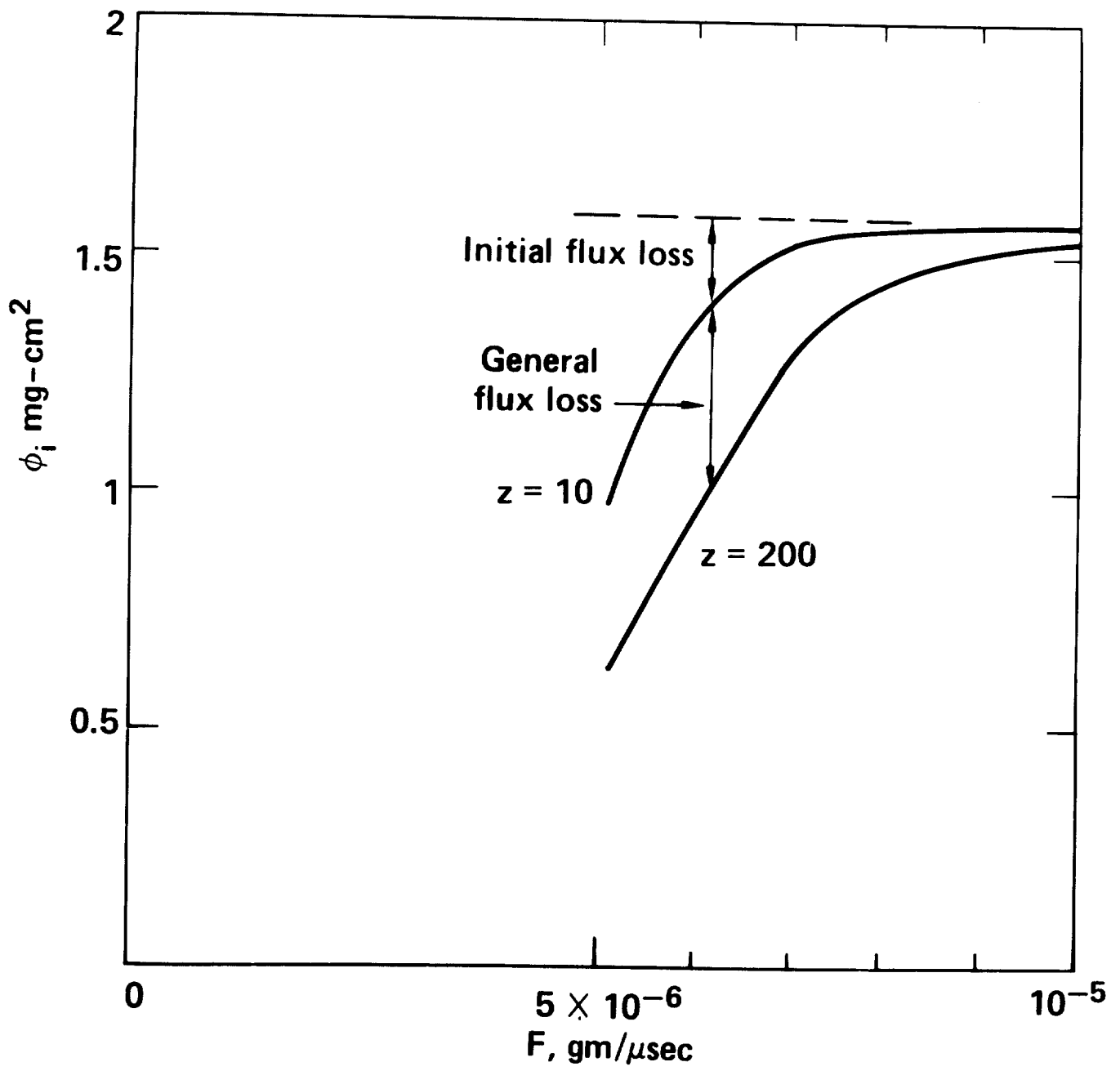


Figure 4

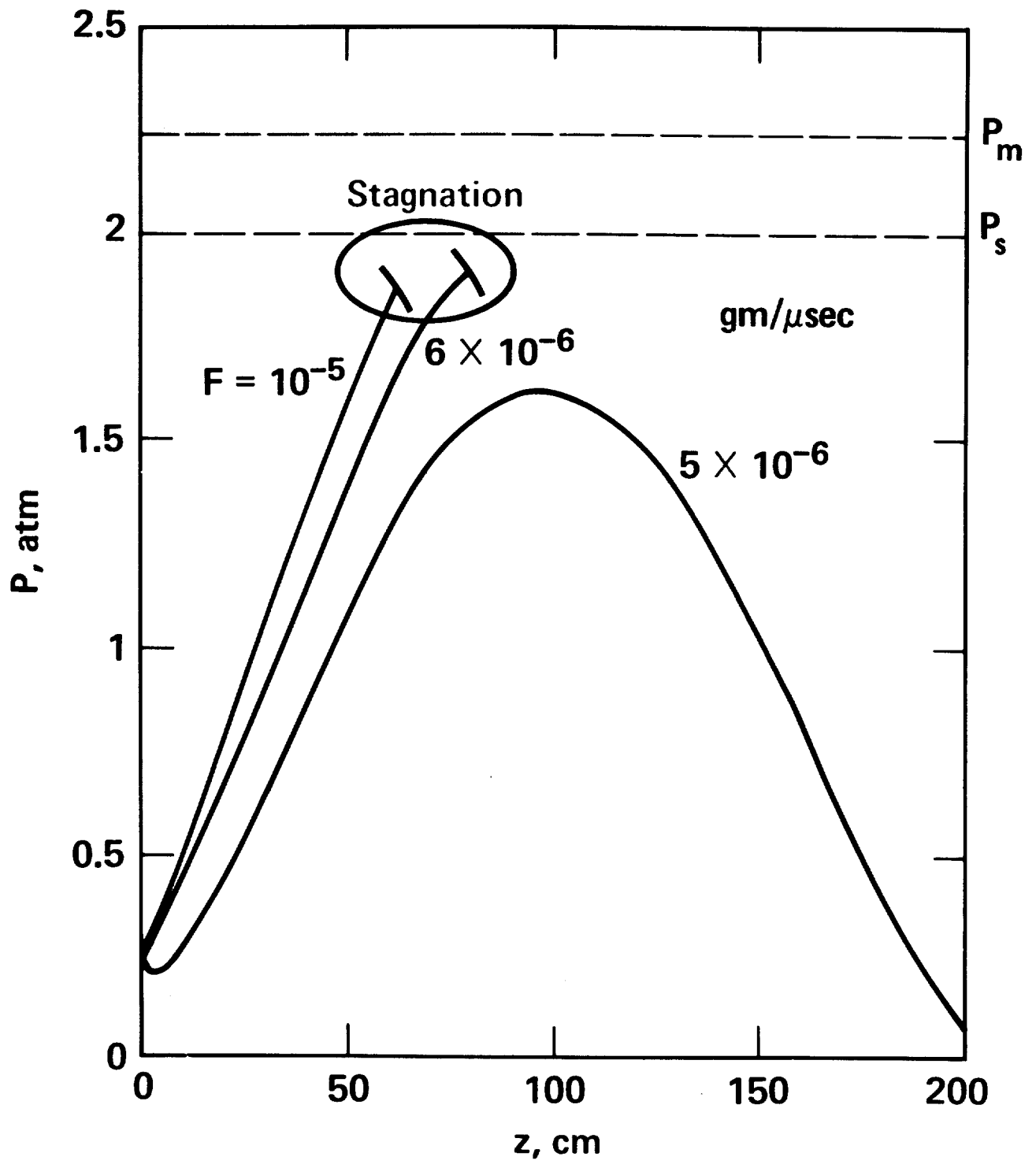


Figure 5

$$\phi_i = 1.0 \text{ MG-cm}^2$$

$$\phi_0 = 14.1 \sin \frac{\pi}{2} (t - 10.4)$$

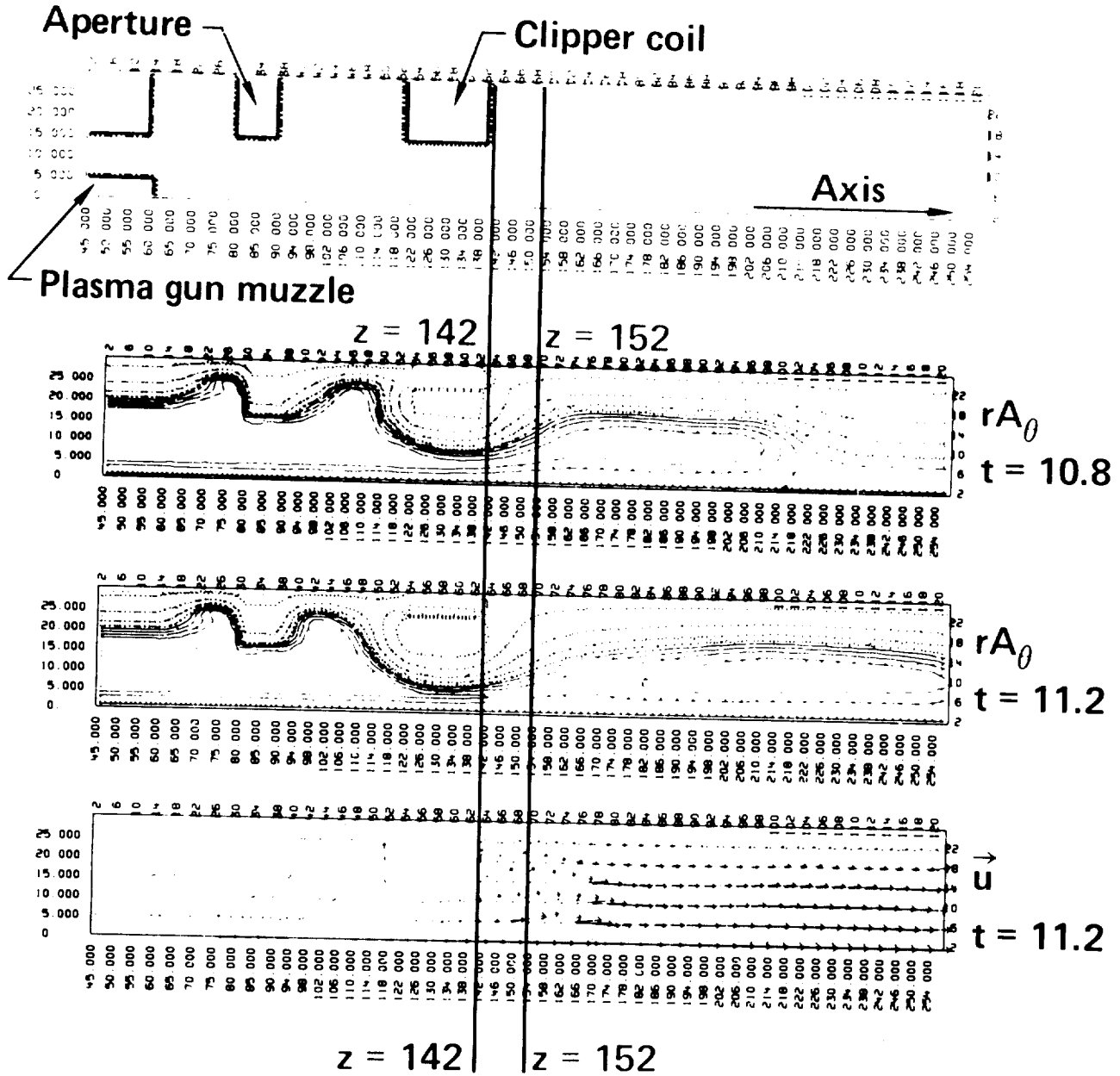


Figure 7